Paper No.
16964

CORROSION 2021 Virtual Conference & Expo April 19-30

AMPP Association for Materials Protection & Performance

A Quantitative Study of $FeCO_3$ Solubility in Non-ideal Solutions

Xin Gao, Fazlollah Madani Sani, Zheng Ma, Bruce Brown, Marc Singer, Srdjan Nesic
Institute of for Corrosion and Multiphase Technology
Ohio University
342 West State Street
Athens, OH 45701

ABSTRACT

The effect of NaCl concentration (non-ideality) was investigated on the solubility of $FeCO_3$ layer. After a layer of $FeCO_3$ was formed on a gold coated crystal, NaCl was incrementally added into the solution and the mass change of the $FeCO_3$ layer was measured with an Electrochemical Quartz Crystal Microbalance (EQCM). It was found that the mass of the precipitated $FeCO_3$ layer did not change with increasing NaCl concentration even though the saturation value of $FeCO_3$ (S_{FeCO_3}.) was far below 1 and dissolution of $FeCO_3$ was expected. It was hypothesized that the calculation of S_{FeCO_3} was incorrect due to inaccurate equations for dissociation equilibrium constants or solubility product constant (K_{sp}). Therefore, the equations for dissociation equilibrium constants taken from Oddo & Tomson 1982 and the K_{sp} equation borrowed from Sun et al. 2009 were revisited. New equations were proposed for carbonic acid first dissociation equilibrium constant (K_{ca}) and K_{sp}.

$$K_{ca} = 387.6 \times 10^{-(6.527-1.594\times10^{-3}T_f+8.52\times10^{-6}T_f^2-3.07\times10^{-5}P-0.7173I^{0.5})}$$

$$K_{sp} = 10^{-(58.98+0.041377T_K+\frac{2.1963}{T_K}-24.5724\,log\,T_K-1.5223I^{0.5}+0.5594I)}$$

The predicted pH and S_{FeCO_3} values at low pressures over a temperature range of 30°C to 80°C and an ionic strength range of 0 to 4.95 M were in good agreement with the experimental results. The new equations could justify the observations for the effect of NaCl concentration on $FeCO_3$ solubility.

Keywords: Iron carbonate layer, $FeCO_3$ solubility, non-ideal solutions, ionic strength, salt concentration, water chemistry model

INTRODUCTION

Iron carbonate ($FeCO_3$) formed on the internal surface of oil and gas pipelines plays an important role in protecting these pipelines from further corrosion. Whether precipitation of $FeCO_3$ is thermodynamically favorable is determined by a parameter called saturation of $FeCO_3$, S_{FeCO_3}. In CO_2 corrosion, ferrous ions, coming from the dissolution of the steel matrix, combine with carbonate ions to form $FeCO_3$. Precipitation of $FeCO_3$ occurs when S_{FeCO_3} is larger than one. If the precipitated $FeCO_3$ covers the steel surface evenly, it can form a compact and protective layer. This acts as a diffusion barrier hindering the mass transfer of corrosive species to the surface, which enhances the resistance of mild steel to further uniform CO_2

corrosion. S_{FeCO_3} is inversely proportional to the $FeCO_3$ solubility limit constant, K_{sp}. Therefore, it is important to be able to calculate K_{sp} accurately, which is a function of temperature and ionic strength. There are several studies that investigated the effect of temperature [1–3] and ionic strength [4] on K_{sp}. When Sun, *et al.* [5] reviewed literature associated with $FeCO_3$ solubility, they found studies of K_{sp} at room temperature and very low ionic strength, studies of solubility limit dependence on temperature, as well as studies of solubility limit dependence on ionic strength. Sun et al. combined the equations from Greenberg and Tomson [2] for temperature† and Silva et al. [4] for ionic strength‡ to obtain a new equation for calculating the iron carbonate solubility product constant as a function of both temperature and ionic strength as follows:

$$logK_{sp} = f(T_K) + f(I) \; = \; -59.3498 - 0.041377 \times T_K - \frac{2.1963}{T_K} + 24.5724 \times log(T_K) + 2.518 \times I^{0.5} - 0.067 \times I \quad (1)$$

Where T_K is temperature in Kelvin and I is ionic strength in mol/L.

They claimed that the new proposed equation agreed well with experimental data. However, as will be shown in this article, Sun et al.'s equation is only valid for low ionic strengths and does not yield to correct predictions of K_{sp} in concentrated brines that are often encountered in the field. Therefore, it is necessary to calculate K_{sp}§ accurately to be able to understand better CO_2 localized corrosion caused by partial dissolution of $FeCO_3$. Two approaches can be followed to obtain K_{sp}. The first approach is to use concentrations for calculating the saturation index (S_{FeCO_3}(Eq. (2)), assuming ideality of the aqueous solution. The second approach is to use activities (product of concentrations and activity coefficients) for S_{FeCO_3} calculations as shown by Eq. (3)**. Although the second approach will be more accurate, it requires the use of complicated water chemistry models such as those proposed by Pitzer et al. [6,7], and Li and Duan [8] to calculate the concentrations and corresponding activity coefficients. However, if K_{sp} in Eq. (1) is defined accurately as a function of both temperature and ionic strength, then concentrations can be used to calculate S_{FeCO_3}which makes the whole calculation much easier.

$$S_{FeCO_3} = \frac{c_{Fe^{2+}}(T,P) \cdot \; c_{CO_3^{2-}}(T,P)}{K_{sp}(T,I)} \quad (2)$$

$$\boldsymbol{S_{FeCO_3} = \frac{a_{Fe^{2+}} \cdot a_{CO_3^{2-}}}{K_{sp}(T)} = \frac{(c_{Fe^{2+}}(T,P) \cdot \gamma_{Fe^{2+}}(T,P,I)) \cdot (c_{CO_3^{2-}}(T,P) \cdot \gamma_{CO_3^{2-}}(T,P,I))}{K_{sp}(T)}} \quad (3)$$

When $S_{FeCO_3} > 1$, $FeCO_3$ forms and precipitates in solution. When $S_{FeCO_3} = 1$, the $FeCO_3$ precipitation rate is equal to the dissolution rate and the system is in equilibrium. Accordingly, the mass of a precipitated layer should not change over time at equilibrium and should begin to dissolve when $S_{FeCO_3} < 1$.

The purpose of this study is to obtain an accurate equation for K_{sp} as a function of both temperature and ionic strength for calculating S_{FeCO_3} in order to be able to analyze $FeCO_3$ precipitation. To reach this goal, the equilibrium constant equations for carbonic acid dissociation proposed by Oddo and Tomson [9] will be revisited first to ensure a correct speciation calculation. After that, a very accurate technique, EQCM (Electrochemical Quartz Crystal Microbalance), will be employed to measure the $FeCO_3$ precipitation, so that the accuracy of the obtained K_{sp} equation can be validated.

† Valid from 25°C to 94°C.
‡ Valid from 0.1 to 5.5 mol/L at 25°C
§ The pressure dependency of K_{sp} is negligible and therefore it is not considered here.
** Activity of $FeCO_3$ is considered to be 1.

Reactions and Equilibrium Constant in H_2O-NaCl-CO_2 system

In the present study, the system of interest is an open system in which CO_2 gas, at a constant partial pressure, is in contact with an aqueous NaCl solution. It can be assumed that the solution is saturated with CO_2. When iron is exposed to this system and corrodes, ferrous irons will be introduced in the solution. Ferrous and carbonate ions can react to form $FeCO_3$ if $S_{FeCO_3} > 1$. For this, the equilibrium concentration of CO_3^{2-} is needed.

The occurring reactions in our system are listed in Table 1. This paper will take the first approach (Eq. (2)) to obtain K_{sp} since it is more convinient and could provide as good predictions when the equations are correct.

Table 1 Main chemical reactions occurring in an aqueous CO_2 solution and corresponding equilibrium constants expression

Reactions		Equilibrium constant	Reaction #
CO_2 Dissolution	$CO_{2(g)} \overset{K_{sol}}{\Longleftrightarrow} CO_{2(aq.)}$	$K_{sol} = c_{CO_{2(aq)}}/P_{CO_2}$	(4)
CO_2 hydration	$CO_{2(aq)} + H_2O \overset{K_{hyd}}{\Longleftrightarrow} H_2CO_{3(aq)}$	$K_{hyd} = c_{H_2CO_3}/c_{CO_{2(aq)}}$	(5)
Carbonic acid dissociation	$H_2CO_{3(aq)} \overset{K_{ca}}{\Longleftrightarrow} H^+{}_{(aq)} + HCO^-_{3(aq)}$	$K_{ca} = c_{H^+}c_{HCO_3^-}/c_{H_2CO_3}$	(6)
Bicarbonate ion dissociation	$HCO^-_{3(aq)} \overset{K_{bi}}{\Longleftrightarrow} H^+{}_{(aq)} + CO^{2-}_{3(aq)}$	$K_{bi} = c_{H^+}c_{CO_3^{2-}}/c_{HCO_3^-}$	(7)
Water dissociation	$H_2O_{(l)} \overset{K_{wa}}{\Longleftrightarrow} H^+_{(aq)} + OH^-_{(aq)}$	$K_{wa} = c_{H^+}c_{OH^-}$	(8)
Iron carbonate precipitation	$Fe^{2+}{}_{(aq)} + CO^{2-}_{3(aq)} \overset{1/K_{sp}}{\Longleftrightarrow} FeCO_{3(s)}$	$K_{sp} = C_{Fe^{2+}}C_{CO_3^{2-}}$	(9)

c_i is the concentration of i.

It is important to mention that, for Eq. (9), $C_{Fe^{2+}}$ is not the total bulk $C_{Fe^{2+}}$ (measured by the spectrophotometer) in the solution because when NaCl is present in the system, the formation of ferrous chloride complexes should be considered [10],

$$Fe^{2+}{}_{(aq)} + Cl^-{}_{(aq)} \overset{K_1}{\Leftrightarrow} FeCl^+{}_{(aq)} \tag{10}$$

The formation of $FeCl^+$ decreased the available $C_{Fe^{2+}}$ for $FeCO_3$ precipitation. $C_{Fe^{2+}}$ can be calculated as follows:

$$C_{Fe^{2+}} = C_{Fe^{2+},\ measured} - C_{FeCl^+} \tag{11}$$

To find out the equilibrium concentrations of CO_3^{2-}, the equilibrium constants for the reactions listed in Table 1 are needed. These equations, mentioned earlier in the introduction, are taken from Oddo and Tomson [9] and Kharaka [11] publications. Table 2 lists these equations.

Table 2 The empirical equations for the equilibrium constants

Equilibrium constant	Unit	Equation #	Ref
$K_{sol} = 14.46 \times 10^{-(2.27+5.65\times10^{-3}T_f-8.06\times10^{-6}T_f^2+0.075\times I)}$	molar/bar	(12)	9
$K_{hyd} = 2.58 \times 10^{-3}$	-	(13)	12
$K_{ca} = 387.6 \times 10^{-(6.41-1.594\times10^{-3}T_f+8.52\times10^{-6}T_f^2-3.07\times10^{-5}P-0.4772I^{0.5}+0.118I)}$	molar	(14)	9
$K_{bi} = 10^{-(10.61-4.97\times10^{-3}T_f+1.33\times10^{-5}T_f^2-2.624\times10^{-5}P-1.166I^{0.5}+0.3466I)}$	molar	(15)	9
$K_{wa} = 10^{-(29.3868-0.0737549T_k+7.47881\times10^{-5}T_k^2}$	molar^2	(16)	11
$K_{sp} = 10^{-59.3498-0.041377\times T_K-\frac{2.1963}{T_K}+24.5724\times log(T_K)+2.518\times I^{0.5}-0.067\times I}$	molar^2	(17)	5
$K_1 = 10^{-(-7.1783+\frac{911.13}{T_k}+0.013407T_k)}$	1/molar	(18)	10

T_f is temperature in Fahrenheit, T_k is absolute temperature in Kelvin, $I = \frac{1}{2}\sum_i c_i z_i^2$ is ionic strength in molar, and P is total pressure in psi.

In the current system, a known concentration of Fe^{2+} was injected to adjust the S_{FeCO_3}. Four equations are needed to solve for the four unknown concentrations (H^+, OH^-, HCO_3^-, CO_3^{2-}). Besides the three equations listed in in Eqs. (14), (15) and (16), the solution was always electroneutral, which leads to the fourth equation:

$$C_{H^+} + 2C_{Fe^{2+}} + C_{Na^+} = C_{HCO_3^-} + 2C_{CO_3^{2-}} + C_{Cl^-} + C_{OH^-} \quad (19)$$

The bulk solution pH and concentrations of all the aqueous species can be calculated from the above equations. And the bulk solution pH can also be measured by a pH meter.

EXPERIMENTAL PROCEDURE

Experimental Setup

In order to study the effect of salt concentration on $FeCO_3$ layer precipitation, an EQCM, designed and manufactured by Stanford Research Systems††, was used to monitor the *in-situ* mass change caused by $FeCO_3$ precipitation/dissolution on the specimen surface. A gold coated EQCM crystal was used in the experiments because Au is inert under the experimental conditions, and so any mass change captured by the EQCM was only caused by $FeCO_3$ precipitation/dissolution. Experiments were carried out in a 2-liter glass cell with three electrodes as shown in Figure 1a. In order to exclude a possible oxygen effect on corrosion, the solution was sparged with CO_2 at least two hours before the experiment and the sparging remained for the entire experiment duration. A special container (Figure 1b) was implemented to remove O_2 from the dry NaCl crystals when adding the extra NaCl during the experiment. The gold coated quartz crystal was polarized cathodically to -700 mV vs. Ag/AgCl to simulate the corrosion potential of mild steel in CO_2 environments.

†† Trade Name

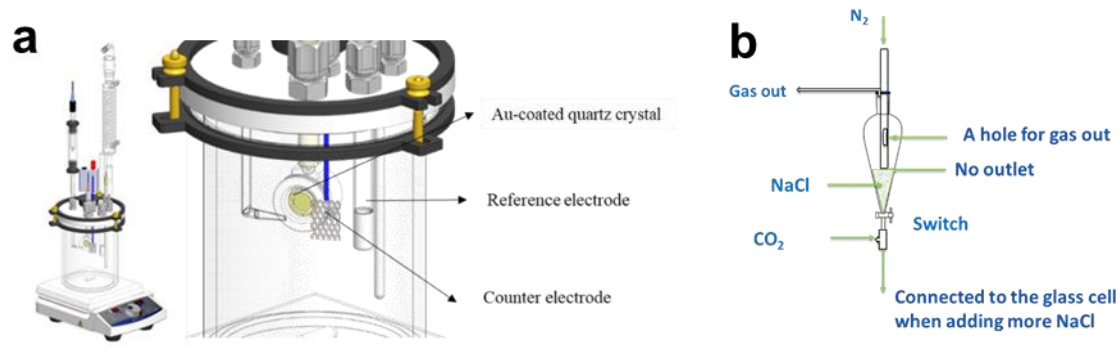

Figure 1. (a) Experimental setup with EQCM (Image courtesy of Cody Shafer, ICMT) [17] (b) Specially designed container for adding NaCl into the glass cell

Experimental Procedure

Each experiment had three stages: (1) $FeCO_3$ layer formation, (2) set $S_{FeCO_3} = 1$, and (3) addition of NaCl to the solution. At stage one, 20.2 g NaCl and 2 L DI water were added into the glass cell to make 1 wt.% NaCl solution, and 2.62 g $NaHCO_3$ to adjust pH value to 6.6. The solution was sparged with CO_2 for at least 2 h to remove oxygen and saturate the solution with CO_2. Then, 100 ppm total Fe^{2+} was injected into the glass cell to produce a super saturation condition with respect to $FeCO_3$ (S_{FeCO_3} >> 1). For stage two, the bulk pH was adjusted at 5.0 by adding 1N HCl to the system to make the S_{FeCO_3} stable at 1. In the stage three, NaCl was added to the solution to study the effect of NaCl concentration on solubility of $FeCO_3$ layer. Six final NaCl concentrations of 3, 5, 10, 15, 20, and 25 wt.% were tested. $C_{Fe^{2+}}$ was measured periodically during each experiment by an HACH‡‡ DR 3000 spectrophotometer.

For all three stages, to calculate S_{FeCO_3}, the total bulk $C_{Fe^{2+}}$ was measured, and available $C_{Fe^{2+}}$ was calculated by Eqs. (11) and (18), $C_{CO_3^{2-}}$ was calculated from Eqs. (12)-(16), and K_{sp} was calculated using Eq. (17). Finally, Eq. (2) was employed to compute S_{FeCO_3}.

Experimental Conditions

The test conditions for the experiments at stage 1 associated with aqueous equilibrium of $FeCO_3$ on Au-coated crystals is shown in Table 3.

Table 3 Experimental conditions for the first stage of the experiment

Total pressure/bar	1
Sparge gas	CO_2
Temperature/°C	80
Initial solution pH	6.6
EQCM crystal	Etched Au-coated quartz crystal
Initial total [Fe^{2+}]/ppm	~100
Initial solution	1 wt.% NaCl
Polarization /mV vs. Ag/AgCl	-700

RESULTS AND DISCUSSION

Stage one: Iron Carbonate Layer Formation

The mass change monitored by EQCM is shown in Figure 2. In the first two hours, the mass increased quickly from 0 to around 450 μg/cm^2 due to the precipitation of $FeCO_3$ on the quartz crystal. A liquid

‡‡ Trade Name

sample (2 ml) was taken out of the glass cell for measuring $C_{Fe^{2+}}$ and solution pH was recorded at the same time. As shown in Figure 2a, S_{FeCO_3} decreased dramatically from 400 (at beginning of the experiment) to around 230 with $FeCO_3$ formation in the first two hours. According to Reaction (9), CO_3^{2-} was consumed during the formation of $FeCO_3$, and therefore, Reactions (5), (6), and (7) proceeded forwards and more H^+ was produced. As a result, the solution pH decreased during the formation of $FeCO_3$ as shown in Figure 2b.

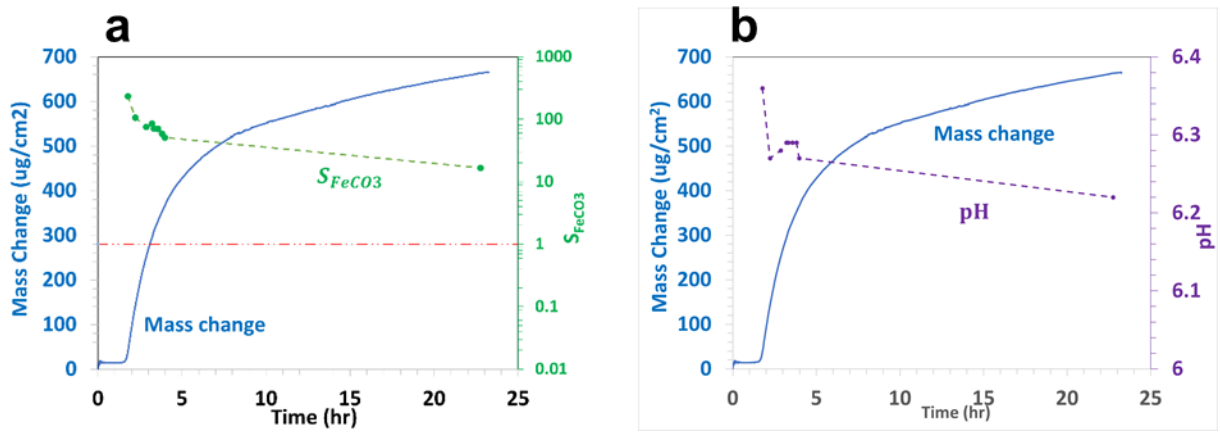

Figure 2. Variation in the mass of $FeCO_3$ precipitation on a polarized Au-coated quartz crystal measured by an EQCM and: (a) the corresponding S_{FeCO_3} (b) pH obtained on at 80°C and 1 wt.% NaCl for stage one

Stage Two: Set $S_{FeCO_3} = 1$

As shown in Figure 2a, after 24 hours of $FeCO_3$ buildup, S_{FeCO_3} decreased to 16.7. However, this value was still greater than 1, which means that the system had not reached equilibrium (S_{FeCO_3}= 1). Therefore, deoxygenated HCl 1N was added to the system dropwise to lower the pH and adjust S_{FeCO_3} to 1. As shown in Figure 3b, with the addition of HCl, the pH decreased immediately, and the mass change decreased simultaneously because part of the iron carbonate dissolved and led to an increase in $C_{Fe^{2+}}$ and $C_{CO_3^{2-}}$. However, with the decrease in pH, Reaction 7 moved to the left and S_{FeCO_3} decreased. The final effect of decrease in solution pH was a decrease in S_{FeCO_3} which was calculated using the equations mentioned above. Finally, when the pH was adjusted to 5.0 at approximately 26 hours after the beginning of the experiment, S_{FeCO_3} was calculated to be 0.2, smaller than 1. At this point, $FeCO_3$ partially dissolved as expected and produced more Fe^{2+}. Then S_{FeCO_3} increased gradually and reached around 1 after 45 hours from the beginning of the experiment. The same trend was reported by Yang[14].

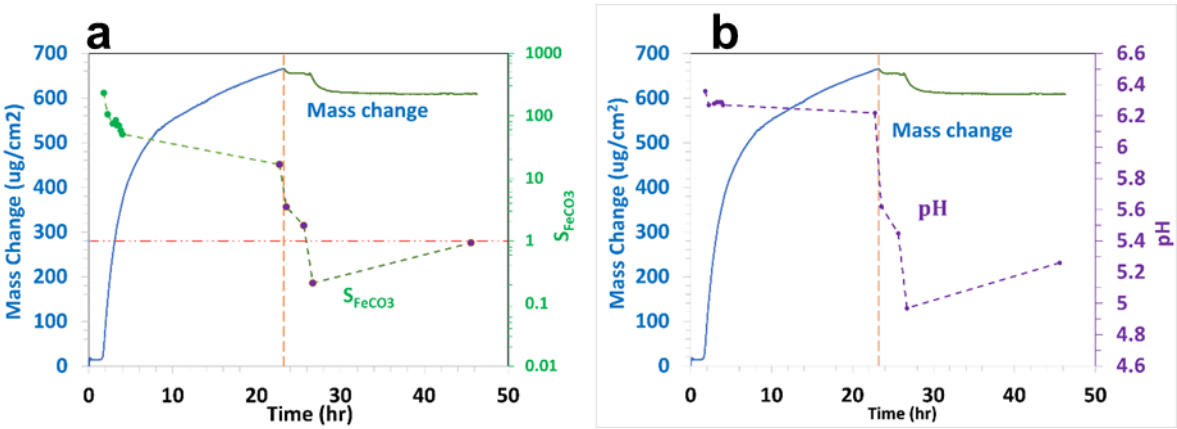

Figure 3. Variation in the mass of $FeCO_3$ precipitation on a polarized Au-coated quartz crystal measured by an EQCM and: (a) the corresponding S_{FeCO_3} (b) pH obtained on at 80°C and 1 wt.% NaCl (pH adjusted from pH 6.3 to pH 5.0 at 22 hours)

Stage Three: Study the Effect of NaCl Concentration on $FeCO_3$ Solubility

After 24 hours, the mass and pH were stable and S_{FeCO_3} returned to 1, which meant that the system reached equilibrium from the previous condition. Then, additional NaCl was added into the system to increase the accumulated [NaCl] to 3 wt.%. The change of mass and S_{FeCO_3} after changing [NaCl] are shown in Figure 4a, while the change of mass and bulk solution pH is shown in Figure 4b.

As shown in Figure 4, upon adding NaCl, the first measurement taken within one hour showed that the EQCM mass decreased only slightly from 610 to 608 µg/cm^2 while the solution pH decreased from 5.26 to 5.18, and S_{FeCO_3} decreased from 0.9 to 0.3. After 5 hours, the EQCM mass remained stable at 603 µg/cm^2. The pH increased slightly to 5.24, which is close to the pH value of 5.26 before adding the NaCl; S_{FeCO_3} was still calculated to be ~0.4. During the 5 hours after adding NaCl, the EQCM mass and pH appeared to be steady, which meant the system reached equilibrium again and had no dramatic difference from the previous state.

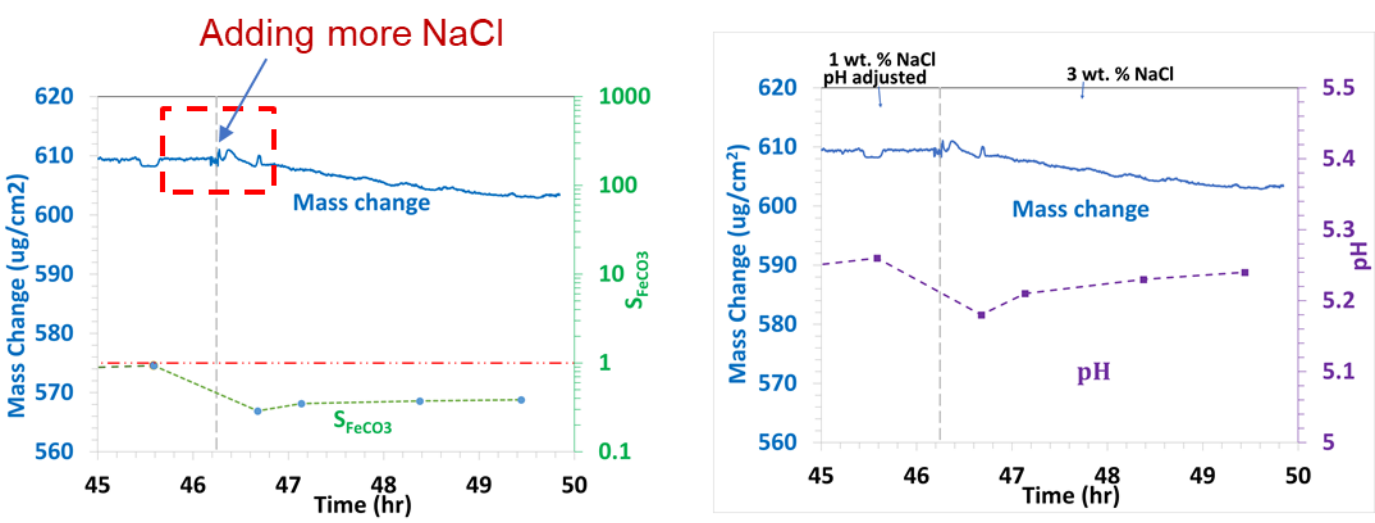

Figure 4. Variation in the mass of $FeCO_3$ precipitation on a polarized Au-coated quartz crystal measured by an EQCM: (a) the corresponding S_{FeCO_3} (b) pH when NaCl concentration was increased from 1 wt.% to 3 wt.%

The mass change, pH and S_{FeCO_3} change associated with the polarized Au-coated quartz crystal for the entire experimental duration are displayed in Figure 5 and Figure 6. The system recovered to an equilibrium condition for each NaCl concentration. It is indicated that mass change had only 0.6% change (4 µg/cm^2 within around 200 hours) from the end of pH adjustment at 1 wt.% NaCl (at around 46 hours) to 25 wt.% NaCl. The pH change shows a downward trend in Figure 6, which could be due to an increased [H^+] caused by the increase activity coefficient of H^+ [15]. However, it should be noted that the system reached equilibrium when the calculated S_{FeCO_3}, based on K_{sp} from Eq. (17) and Kca from Eq. (14), was much less than 1. This is in conflict with the theory explained in the introduction. Therefore, it was hypothesized that the calculation of saturation value was incorrect and Eqs. (17) and (14) need to be modified to fix this.

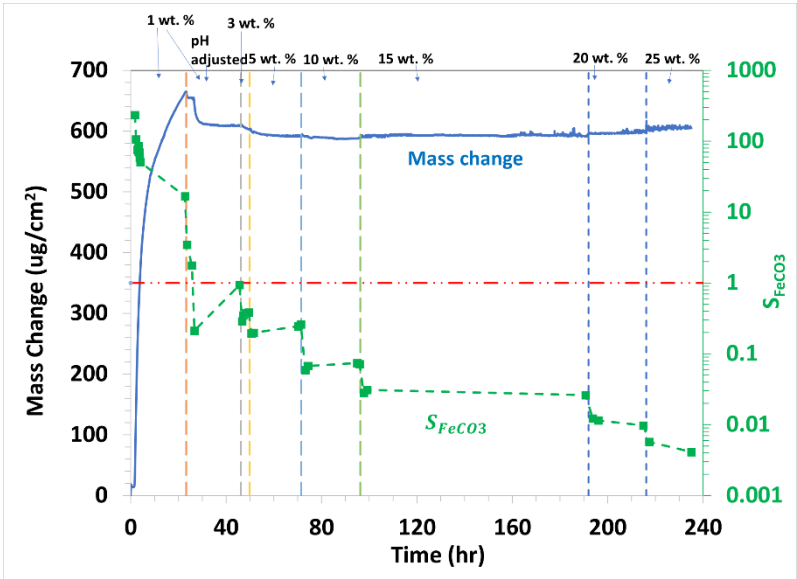

Figure 5. Variation in the mass of $FeCO_3$ precipitation on a polarized Au-coated quartz crystal measured by an EQCM and the corresponding S_{FeCO_3} when NaCl concentration was increased

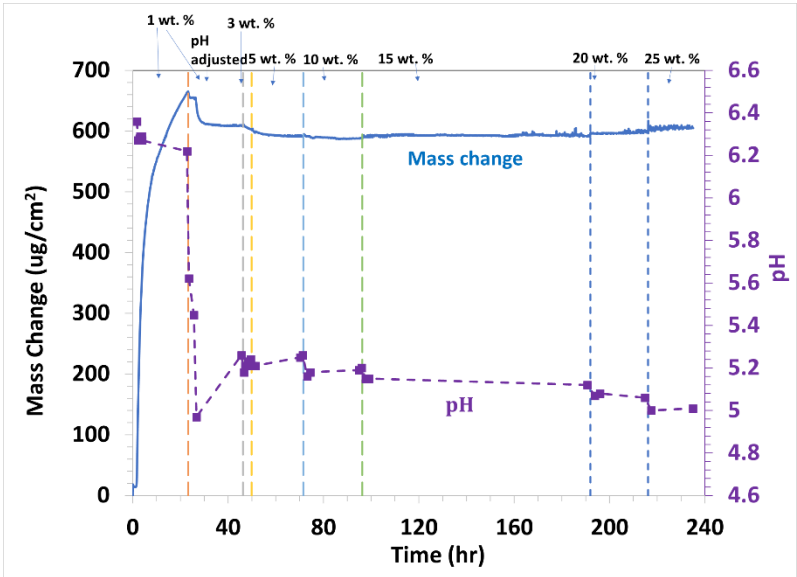

Figure 6. Variation in the mass of $FeCO_3$ precipitation on a polarized Au-coated quartz crystal measured by an EQCM and the corresponding pH when NaCl concentration was increased

Comparison of Predicted and Experimental pH Values in H_2O-NaCl-CO_2 System

The wrong S_{FeCO_3} values could be because of an inaccurate equation for the dissociation equilibrium constants (Eqs. (12)-(16)) or for K_{sp} (Eq. (17)) or both. To find out about the former possibility, the measured pH values at 1 bar total pressure and three temperatures were compared with those predicted by the Oddo & Tomson model which was used to calculate S_{FeCO_3} and another model based on Li and Duan publication [16]. The Li & Duan model reproduced by F. Madani Sani as part of his Ph.D. research [15] is a thermodynamic water chemistry model for the H_2O-NaCl-CO_2 system that allows calculating the equilibrium concentrations and activity coefficients of dissolved species in a temperature range of 0-250°C, pressure range of 0-1000 bar, and NaCl concentration range of 0-5 molality [16]. In Figure 7a at 80°C, the purple dots signify the measured pH values; the blue line shows the predicted pH values from Oddo & Tomson model (Eqs. (12) – (16)); the green line displays the pH calculated from Li & Duan model. From 0.1 wt.% to 5 wt.% NaCl, both Oddo & Tomson and Li & Duan models predicted similar pH values and they were close to the experimental pH values. However, with further increase in NaCl concentration, the Oddo & Tomson model exhibited a large deviation from the measured pH, while the predictions from the Li & Duan model were much closer to the measured values. The same comparisons were observed at 50°C (Figure 7b) and 30°C (Figure 7c). Therefore, the equations for the dissociation equilibrium constants based on the Oddo & Tomson model need to be revised.

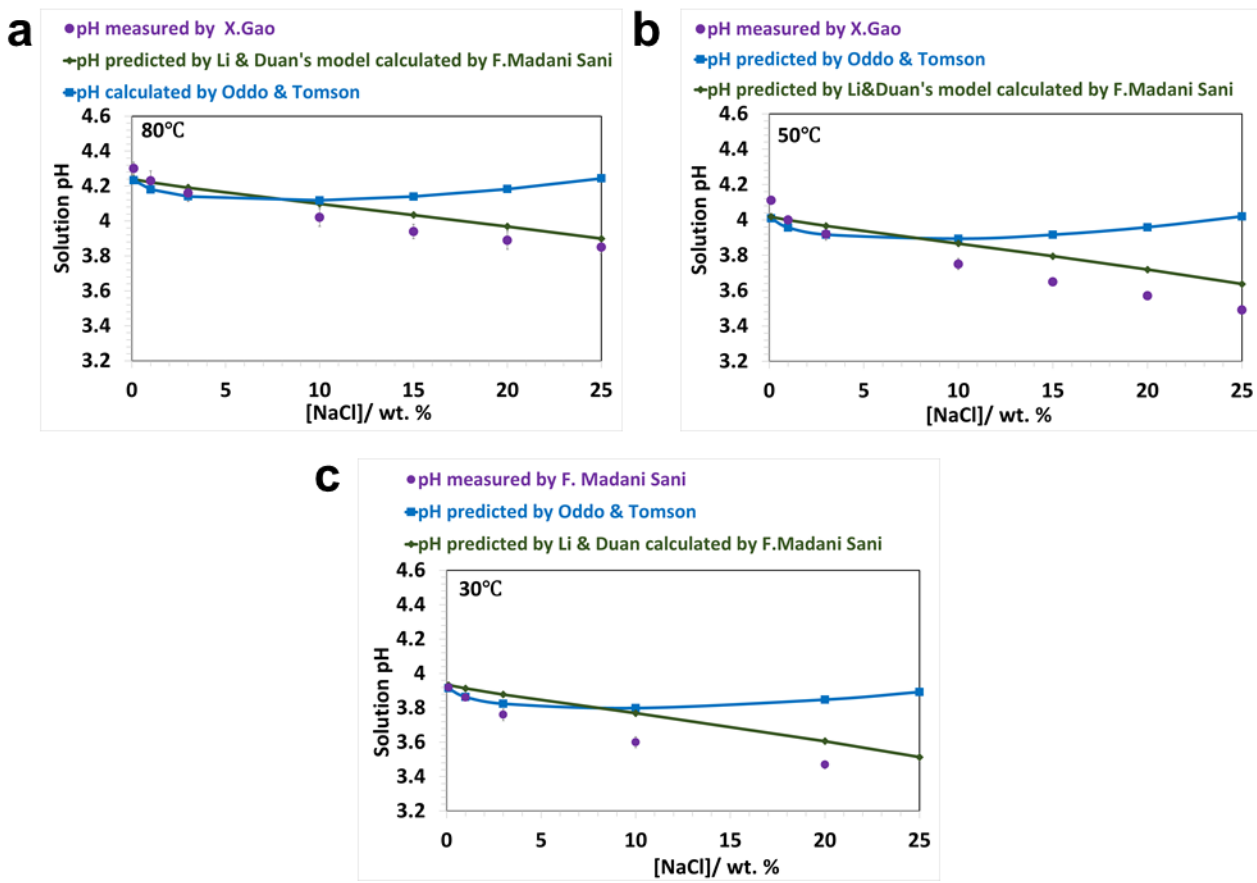

Figure 7. Comparison of the predicted and the measured pH values at different NaCl concentrations and: (a) 80°C (b) 50°C (c) 30°C

MODEL REVISION AND VALIDATION

Revision of the Oddo & Tomson Water Chemistry Model

Among the four equilibrium constants of K_{sol}, K_{hyd}, K_{ca} and K_{bi}, the hydration constant, K_{hyd}, does not change with ionic strength (NaCl concentration). Therefore, there is no need to revise K_{hyd}. For other

three constants of K_{sol}, K_{ca} and K_{bi} it will be too complicated to revise them altogether. Therefore, each needs to be reviewed separately, while the other two constants are kept unchanged.

Figure 8 shows CO_2 solubility in aqueous NaCl solutions as a function of ionic strength calculated by K_{sol} equation (Eq. (12)). $C_{CO_{2(aq)}}$ predicted by the Oddo & Tomson model and $C_{CO_{2(aq)}}$predicted by the Duan and Sun CO_2 solubility model [8] are in a good agreement. Since the Duan and Sun model is a very accurate model, K_{sol} equation from the Oddo & Tomson model does not need to be modified.

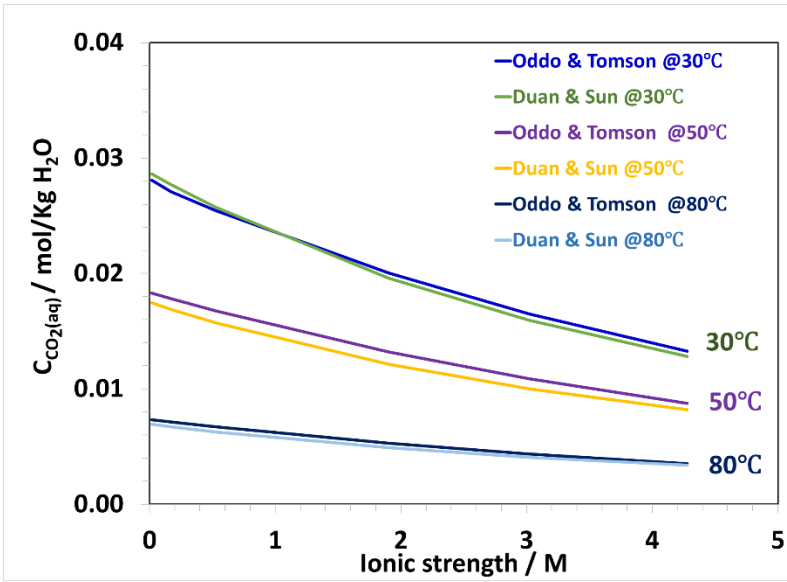

Figure 8. Variation of CO_2 solubility with NaCl concentration in CO_2 saturated NaCl solutions, obtained using the Oddo & Tomson and the Duan and Sun models (reproduced by F. Madani Sani) at 1 bar total pressure and 30°C, 50°C and 80°C.

The ratio of $C_{HCO_3^-}$ to $C_{CO_3^{2-}}$ is approximately 10^5 at 1 bar total pressure in the temperature range of 30°C to 80°C and NaCl concentration range of 0.1 wt.% to 25 wt. %. This ratio reflects that there is a negligible amount of H^+ produced by bicarbonate dissociation (Reaction (7)) as compared to H^+ produced by carbonic acid dissociation (Reaction (6)). This means that the contribution of Reaction (7) in the equilibrium solution pH is negligible and the inaccuracy of K_{bi} equation given in the Odd & Tomson can be neglected.

Consequently, K_{ca}, the carbonic acid dissociation constant, is the one which required modification with respect to the ionic strength. The modified K_{ca} equation was obtained by fitting the best fit line for K_{ca} was determined by Eq. (20):

$$K_{ca} = 387.6 \times 10^{-(6.527-1.594\times10^{-3}T_f+8.52\times10^{-6}T_f^2-3.07\times10^{-5}P-0.7173I^{0.5})} \quad (20)$$

Validation of the New K_{ca} Equation

Figure 9 compares the measured pH values with those obtained using Eq. (20) at 80°C, 50°C, and 30°C are shown in. At 80°C, Li & Duan model predictions have a less than 3% error from the measured data, and the Oddo & Tomson model with the new equation (red line) for K_{ca} resulted in an error less than 4% of the measured data. At 50°C and 30°C, the Oddo & Tomson model with the new equation has a maximum error of 3%, while the error for the Li & Duan model at 30°C is almost 5%.

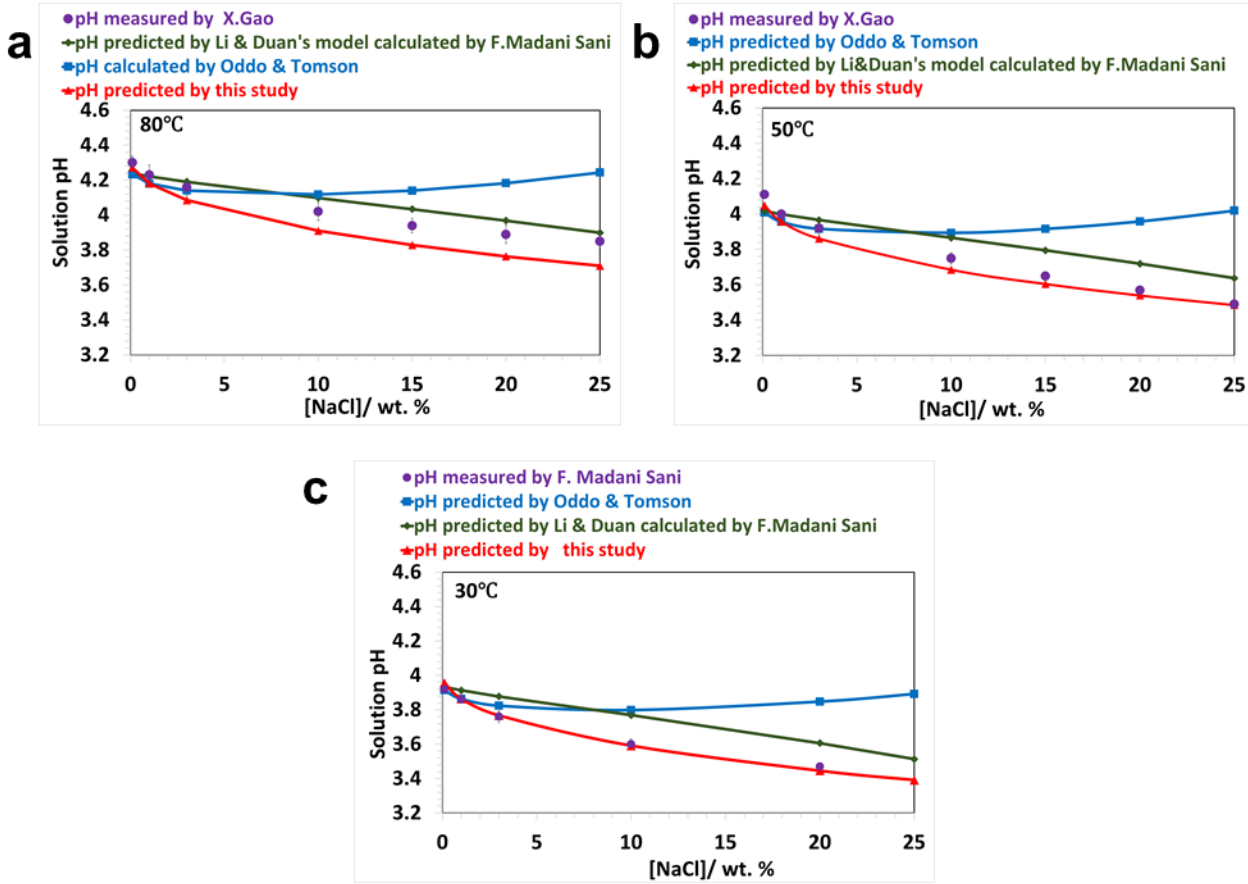

Figure 9. The predicted and measured pH values of CO_2-saturated solutions vs. NaCl concentrations at 1 bar total pressure and: (a) 80°C (b) 50°C (c) 30°C

New K_{sp} Equation Proposed

It was mentioned earlier that when S_{FeCO_3}= 1, the $FeCO_3$ precipitation rate is equal to the $FeCO_3$ dissolution rate and the $FeCO_3$ layer is at equilibrium. Therefore, at the equilibrium conditions, Eq. (2) can be changed to:

$$K_{sp} = C_{Fe^{2+}} C_{CO_3^{2-}} \tag{21}$$

$C_{Fe^{2+}}$ can be measured by spectrophotometer, $C_{CO_3^{2-}}$ and can be back-calculated using Eqs. (4)-(8) and Eqs. (12)-(16) using the measured pH value. Then, K_{sp} can be calculated with Eq. (21). This $K_{sp,}$ is named "experimental K_{sp}".

Figure 10a compared the experimental K_{sp} obtained using Eq. (21) with K_{sp} calculated by the equation proposed by Sun & Nesic model (Eq. (17)). Ideally, all the experimental data should fall onto the blue diagonal line. However, the data points deviate from the diagonal line. Therefore, the K_{sp} equation (Eq. (17)) from Sun & Nesic [5] is not accurate and needs modification with respect to ionic strength.

As part of this research the K_{ca} (Eq. (20)) from Oddo & Tomson's work was modified to provide a more accurate experimental data fitting for the model. Therefore, experimental K_{ca} values were recalculated using Eq. (21) with $C_{CO_3^{2-}}$determined using the new K_{ca} (Eq. (20)). Figure 10b compared the experimental K_{sp} obtained in this study with K_{sp} still calculated by the equation proposed by Sun & Nesic model (Eq. (17)). The data points still deviate from the diagonal line. Therefore, by making slight changes to the

constant term and the coefficients for ionic strength terms in Eq. (17), the best fit to K_{sp} values obtained in this study was determined and a new equation is proposed for K_{sp} as follows:

$$K_{sp} = 10^{-(58.98+0.041377T_K+\frac{2.1963}{T_K}-24.5724\,log\,T_K-1.5223I^{0.5}+0.5594I)} \quad (22)$$

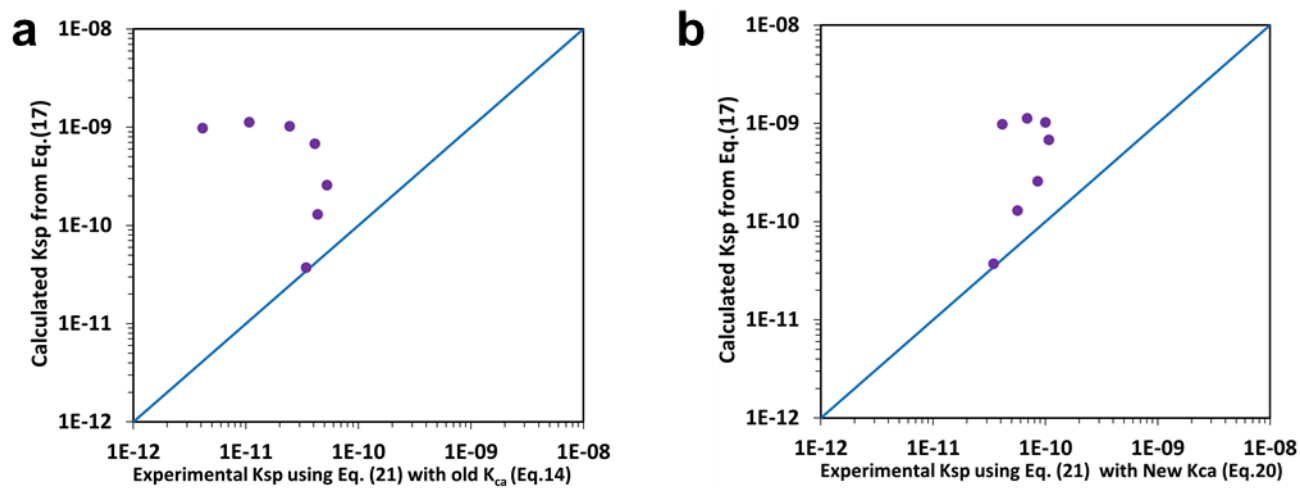

Figure 10. (a) Parity plot comparison of this paper's experimental K_{sp} (Eq. (21), Eq. (14)) vs. calculated K_{sp} from Sun & Nesic [5] model (Eq. (17)) at 80°C (b) Parity plot comparison of experimental K_{sp} (Eq. (21), Eq. (20))vs. K_{sp} from Sun & Nesic [5] model (Eq. (17)) at 80°C

Verification of New Proposed Equation for K_{sp}

Figure 11 shows that using the new equation for K_{sp} results in very good agreement with the K_{sp} values computed based on Fe^{2+} measurements and new K_{ca} Equation.

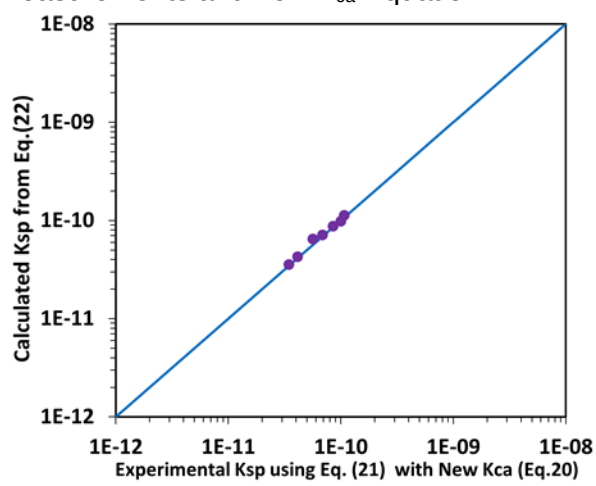

Figure 11. Parity plot comparison of experimental K_{sp} vs. calculated K_{sp} from the new equation (Eq.(22)) at 80°C

As shown in Figure 5, when the system reached the equilibrium condition, the solution saturation was around 1 at lower [NaCl] (1 wt.%). With the increase of the salt concentration, the solution became more under-saturated with respect to $FeCO_3$. Based on the K_{ca} modified model (Eq. (20)), S_{FeCO_3} was

recalculated and is shown in Figure 12. Compared to the saturation value calculated by Sun & Nesic model, the recalculated S_{FeCO_3} values were higher but still unsaturated.

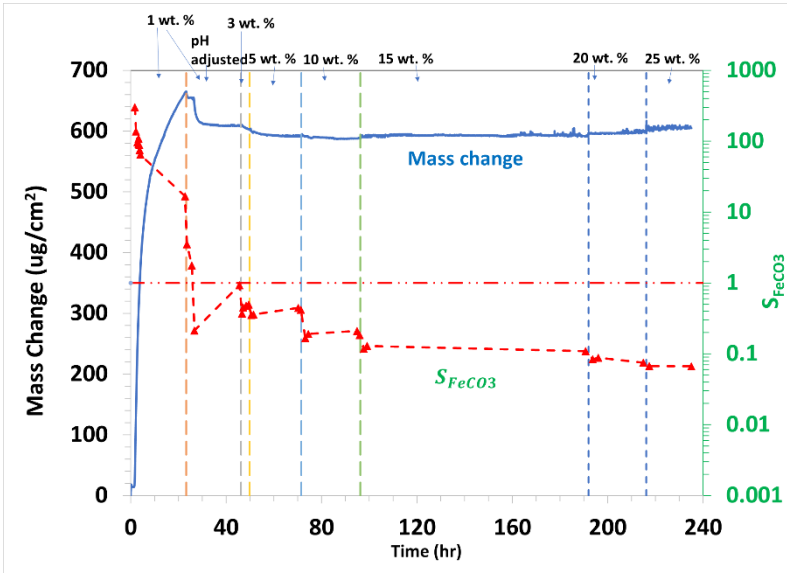

Figure 12. Variation in the mass of $FeCO_3$ precipitation on a polarized Au-coated quartz crystal measured by an EQCM and the corresponding S_{FeCO_3} (recalculated based on K_{ca} adjusted equation, Eq. (20)) when NaCl concentration was increased at 80°C

Recalculated S_{FeCO_3} based on the new proposed K_{sp} equation (Eq. (22)) are plotted in Figure 13. It can be seen that the S_{FeCO_3} decreased initially along with the decrease in solution pH and then increased steadily and reached one after about 20 hours at stage two (pH adjustment). Further addition of NaCl changed S_{FeCO_3} accordingly but the equilibrium S_{FeCO_3} always returned to approximately one after a sufficient amount of time. This agreed with the observation that negligible changes occurred in EQCM measured mass when the system reached equilibrium after each addition of salt. Therefore, it can be concluded that S_{FeCO_3} values shown in Figure 5 were wrong and S_{FeCO_3} almost did not change when NaCl was added to the system. Finally, the EQCM results showed that change in the ionic strength of solution did not have any effect on the solubility of $FeCO_3$ layer. However, this study was done on an Au surface and in more representative conditions where iron is being corroded, salt concentration has a major effect on the CO_2 corrosion process which in turn can be influential on the formation and solubility of $FeCO_3$ layer as well.

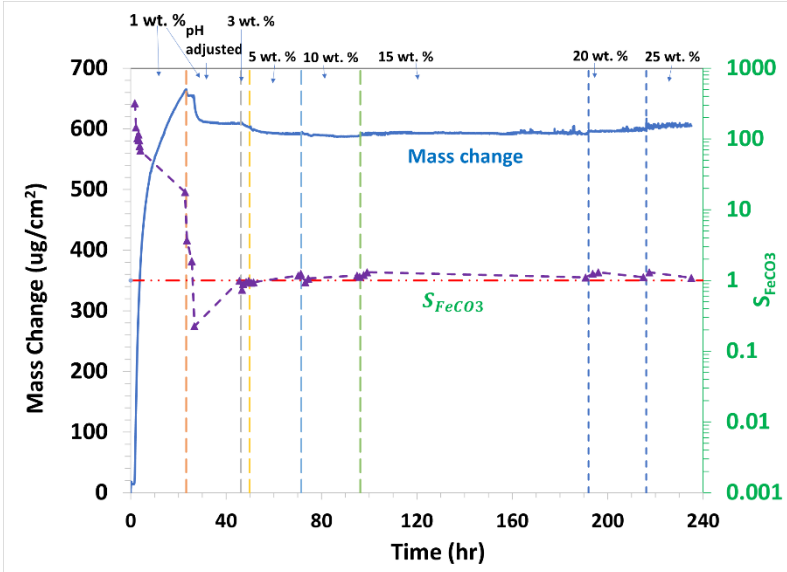

Figure 13. Variation in the mass of $FeCO_3$ precipitation on a polarized Au-coated quartz crystal measured by an EQCM and the corresponding S_{FeCO_3} (recalculated based on K_{ca}, Eq. (20)and K_{sp} adjusted equation, Eq. (22)) when NaCl concentration was increased at 80°C

CONCLUSIONS

- The Oddo & Tomson model was modified to provide more accurate calculations of water chemistry in higher ionic strength solutions without having to use more complicated models that are based on activity coefficients of dissolved species. Predicted pH values by the new equations are in better agreement with measured values at 1 bar total pressure and over the temperature range from 30°C to 80°C and an NaCl concentration range from 0 wt.% to 25 wt.% (0 to 4.95 M)
- Based on EQCM results, a new equation to calculate the solubility constant (K_{sp}) of iron carbonate in non-ideal solutions was developed based on the Sun & Nesic model. Calculated S_{FeCO_3} from the new proposed equation reflects better the K_{sp} values obtained based on experiments and the modified Oddo & Tomson model.
- EQCM measurements showed that adding NaCl to the solution did not change the solubility of $FeCO_3$ layer.

ACKNOWLEDGEMENTS

The author would like to thank the following companies for their financial support: Anadarko, Baker Hughes, BP, Chevron, CNOOC, ConocoPhillips, DNV GL, ExxonMobil, M-I SWACO (Schlumberger), Multi-Chem (Halliburton), Occidental Oil Company, Pioneer Natural Resources, Saudi Aramco, Shell Global Solutions, SINOPEC (China Petroleum), and TOTAL.

REFERENCES

1. Bénézeth, P., Dandurand, J. L. & Harrichoury, J. C. Solubility product of siderite ($FeCO_3$) as a function of temperature (25–250 °C). *Chemical Geology* **265**, 3–12 (2009).
2. Greenberg, J. & Tomson, M. Precipitation and dissolution kinetics and equilibria of aqueous ferrous carbonate vs temperature. *Applied Geochemistry* **7**, 185–190 (1992).
3. Braun, R. D. Solubility of iron(II) carbonate at temperatures between 30 and 80°. *Talanta* **38**, 205–211 (1991).

4. Silva, C. A. R., Liu, X. & Millero, F. J. Solubility of Siderite ($FeCO_3$) in NaCl Solutions. *Journal of Solution Chemistry* **31**, 97–108 (2002).

5. Sun, W., Nesic, S. & Woollam, R. C. The effect of temperature and ionic strength on iron carbonate (FeCO3) solubility limit. *Corrosion Science* **51**, 1273–1276 (2009).

6. Pitzer, K. S. Thermodynamics of electrolytes. I. Theoretical basis and general equations. *J. Phys. Chem.* **77**, 268–277 (1973).

7. PITZER, K. S. Thermodynamics of Aqueous Electrolytes at Various Temperatures, Pressures, and Compositions. in *Thermodynamics of Aqueous Systems with Industrial Applications* vol. 133 451–466 (AMERICAN CHEMICAL SOCIETY, 1980).

8. Duan, Z. & Sun, R. An improved model calculating CO_2 solubility in pure water and aqueous NaCl solutions from 273 to 533 K and from 0 to 2000 bar. *Chemical Geology* **193**, 257–271 (2003).

9. Oddo, J. E. & Tomson, M. B. Simplified calculation of $CaCO_3$ saturation at high temperatures and pressures in brine solutions. *Journal of Petroleum Technology* **34**, 1–583 (1982).

10. Palmer, D. A. & Hyde, K. E. An experimental determination of ferrous chloride and acetate complexation in aqueous solutions to 300°C. *Geochimica et Cosmochimica Acta* **57**, 1393–1408 (1993).

11. Y. K. Kharaka, W. D. Gunter & P. K. Aggarwal. *Solmineq.88; a computer program for geochemical modeling of water-rock interactions*. (1988).

12. Palmer, D. A. & Van Eldik, R. The chemistry of metal carbonato and carbon dioxide complexes. *Chem. Rev.* **83**, 651–731 (1983).

13. Ma, Z., Yang, Y., Brown, B., Nesic, S. & Singer, M. Investigation of precipitation kinetics of $FeCO_3$ by EQCM. *Corrosion Science* **141**, 195–202 (2018).

14. Y. Yang. Removal mechanisms of protective iron carbonate layer in flowing solutions. (Ohio University, 2012).

15. Madani Sani, F., Brown, B., Belarbi, Z. & Nesic, S. An experimental investigation on the effect of salt concentration on uniform CO_2 Corrosion. in.

16. Li, D. & Duan, Z. The speciation equilibrium coupling with phase equilibrium in the H_2O–CO_2–NaCl system from 0 to 250 °C, from 0 to 1000 bar, and from 0 to 5 molality of NaCl. *Chemical Geology* **244**, 730–751 (2007).